Green Valorization of Chromolaena odorata Biomass into Sustainable Cellulose Acetate Butyrate–Zn(OH) 2 Microcapsules for Controlled Antibacterial Release

Jiraporn Ketwaraporn
Uttaradit Rajabhat University
Pongthep Jansanthea
pongthep.jan@uru.ac.th
Uttaradit Rajabhat University
Monthakan Boontheung
Uttaradit Rajabhat University
Suriyun Yimpin
Uttaradit Rajabhat University
Parinya Kraivuttinun
Uttaradit Rajabhat University
Putthadee Ubolsook
Uttaradit Rajabhat University

Research Article

Keywords: Biomass valorization, Biorefinery, Cellulose acetate butyrate, Zinc hydroxide microcapsules, Chromolaena odorata extract, Sustainable antibacterial materials

Posted Date: February 9th, 2026

DOI: https://doi.org/10.21203/rs.3.rs-8052206/v1

Additional Declarations: No competing interests reported.

Abstract

This study presents a green valorization route for *Chromolaena odorata* biomass through the development of sustainable cellulose acetate butyrate–zinc hydroxide (CAB–$Zn(OH)_2$) hybrid microcapsules for controlled antibacterial release. The process integrates renewable plant feedstock and a biodegradable cellulose-derived polymer using an eco-friendly solvent evaporation method, followed by in situ precipitation of $Zn(OH)_2$ under mild aqueous conditions. Structural, morphological, and thermal analyses confirmed the successful formation of $Zn(OH)_2$-coated CAB microcapsules with improved crystallinity, surface roughness, and thermal stability. Antibacterial activity was evaluated against *Escherichia coli* and *Staphylococcus aureus*, revealing that the CAB–Zn–40 formulation exhibited the strongest performance, with minimum inhibitory concentrations of 12.8 mg/mL and 6.4 mg/mL, respectively. The enhanced antibacterial efficacy arises from synergistic interactions between phytochemical constituents of *C. odorata* extract and the sustained release of Zn^{2+} ions, inducing oxidative stress and membrane disruption. This biorefinery-oriented approach demonstrates the conversion of invasive plant biomass into high-value, multifunctional antibacterial materials. The findings highlight a sustainable and scalable pathway for producing bio-based functional composites applicable to wound care, infection-resistant coatings, and active packaging, advancing the principles of circular bioeconomy and environmentally responsible material design.

1. Introduction

The sustainable conversion of renewable biomass into value-added materials has become a central objective in modern biorefinery systems, addressing both resource efficiency and environmental protection. Invasive or underutilized plant species offer abundant, low-cost feedstocks for the production of functional bioproducts within a circular bioeconomy framework [1]. Among the most pressing societal challenges is the growing threat of antimicrobial resistance, which has intensified the search for antibacterial materials that are both effective and environmentally responsible. Conventional synthetic antimicrobials and polymer-based agents often persist in ecosystems, leading to long-term pollution and biological accumulation. As a result, recent research has increasingly emphasized the valorization of biomass into biodegradable polymer systems that incorporate natural antimicrobial agents, achieving safe, long-lasting, and eco-friendly functionality [2, 3].

Plant-derived antimicrobial compounds have emerged as promising alternatives due to their broad-spectrum activity, biocompatibility, and compliance with green chemistry principles. Extracts rich in polyphenols, alkaloids, tannins, and flavonoids exhibit potent antibacterial and antioxidant properties, offering a sustainable pathway for biomass valorization into high-value functional agents. Among these, *Chromolaena odorata* (Siam weed), a rapidly spreading invasive biomass in tropical regions, represents a renewable feedstock suitable for biorefinery applications [4]. Its leaf extract demonstrates significant antibacterial, anti-inflammatory, and wound-healing potential [5]. However, the direct use of such crude extracts limits practical deployment because of their chemical instability, rapid degradation, and lack of controlled release—constraints that reduce long-term efficacy in biomedical and environmental systems [6, 7].

Microencapsulation offers a reliable means of converting plant-derived extracts into stable, controllable delivery systems, protecting sensitive phytochemicals and enabling sustained release [8]. Cellulose acetate butyrate (CAB), derived from lignocellulosic biomass, represents an ideal polymer platform for such

conversion, owing to its tunable permeability, compatibility with natural compounds, and environmental degradability [9]. The integration of CAB into this system aligns with biorefinery strategies for replacing petroleum-based polymers with bio-based, degradable alternatives that reduce waste and environmental burden.

To enhance antibacterial performance, surface functionalization with inorganic agents such as zinc compounds can provide synergistic activity. Zinc-based materials are particularly relevant to sustainable material design because of their natural abundance, biocompatibility, and role in biological systems. While zinc oxide (ZnO) nanoparticles have been extensively used, their rapid ion release and potential cytotoxicity raise ecological concerns [10]. In contrast, zinc hydroxide ($Zn(OH)_2$) provides a controlled Zn^{2+} ion release mechanism that ensures prolonged antibacterial action with reduced toxicity [11]. Nonetheless, integrating $Zn(OH)_2$ coatings with bio-based polymers and plant-derived antimicrobials within a biomass valorization framework remains underexplored.

In this context, the present study contributes to the biorefinery field by demonstrating a green valorization route for *C. odorata* biomass, wherein leaf extract is encapsulated within CAB microcapsules and subsequently coated with $Zn(OH)_2$ via in situ precipitation. This approach merges renewable biomass resources, biodegradable polymer matrices, and eco-benign inorganic coatings to generate multifunctional antibacterial materials. The influence of $Zn(OH)_2$ concentration on the structural, thermal, and antibacterial properties of the resulting hybrids is systematically examined through comprehensive physicochemical characterization. Overall, this work provides a sustainable conversion strategy for transforming invasive biomass into high-value antibacterial materials, advancing the design of environmentally responsible composites for wound care, active packaging, and biorefinery-driven applications.

2. Materials and Biomass Conversion Methods

2.1 Materials

All chemicals used were of analytical grade and employed without further purification. Barium chloride dihydrate ($BaCl_2 \cdot 2H_2O$, ≥ 99.0%) was obtained from Elago Enterprises (Australia). Chloroform ($CHCl_3$, 99.8%) and ethanol (95%) were purchased from RCI LABSCAN (Thailand), while absolute ethanol (99.9%) was obtained from Duksan (Korea). Cellulose acetate butyrate (CAB, Mn ≈ 30,000) and dimethyl sulfoxide (DMSO, 99.9%) were sourced from VWR (UK). Poly(vinyl alcohol) (PVA, analytical reagent grade) was procured from Chem-Supply (Australia), and zinc nitrate hexahydrate ($Zn(NO_3)_2 \cdot 6H_2O$, 98%) from Loba Chemie Pvt. Ltd. (India). Additional chemicals, including sulfuric acid (H_2SO_4, 98%), sodium chloride (NaCl, 99%), and sodium hydroxide (NaOH, 99%), were obtained from RCI LABSCAN. Nutrient broth and agar were supplied by Himedia (India). All aqueous solutions were prepared using deionized (DI) water with a conductivity of < 1 µS/cm.

Fresh *Chromolaena odorata* (Siam weed) leaves were collected from the vicinity of Uttaradit Rajabhat University, Uttaradit Province, Thailand. Leaves were thoroughly washed with DI water to remove debris and microorganisms, air-dried under sunlight for 24–36 hours until fully dehydrated, and then finely chopped to maximize surface area for solvent extraction [12].

2.2 Preparation of C. odorata Leaf Extract

Extraction of bioactive compounds from *Chromolaena odorata* biomass was performed as the initial valorization step in the biorefinery-inspired process. Air-dried leaves were used as lignocellulosic feedstock and extracted with 95% ethanol at a 1:10 (w/v) ratio under ambient conditions (25 ± 2°C) for 24 h with intermittent shaking. The mixture was homogenized, filtered through muslin cloth, and vacuum-filtered using Whatman No. 1 paper.

The filtrate was concentrated under reduced pressure at 45°C and freeze-dried at − 55°C (0.04 mbar) to obtain a stable green powder, rich in polyphenols, alkaloids, and flavonoids with known antibacterial and antioxidant activity [12]. The dried extract was stored in a desiccator and used as the core bioactive component for microencapsulation.

This green ethanol-based extraction provides an eco-efficient route for converting low-value invasive biomass into a high-value bioactive intermediate, consistent with the principles of circular bioeconomy and sustainable biorefinery processing.

2.3 Preparation of CAB-Based Microcapsules

CAB-based microcapsules were fabricated as the core conversion step for integrating biomass-derived extract with a renewable polymer matrix. The process followed green chemistry and biorefinery principles, emphasizing biodegradable materials and low-energy solvent processing.

Cellulose acetate butyrate (CAB) was dissolved in 10 mL of ethyl acetate under magnetic stirring to form a homogeneous solution. The *C. odorata* leaf extract (Section 2.2) was added and stirred for 30 min to ensure uniform dispersion. The organic phase was then emulsified into 50 mL of 1% (w/v) poly(vinyl alcohol) (PVA) solution under moderate stirring (600 rpm) to produce a stable oil-in-water emulsion.

Microcapsules formed via solvent evaporation as CAB precipitated around the encapsulated extract. The suspension was centrifuged at 4,000 rpm for 10 min, washed three times with deionized water, and air-dried at room temperature for 24 h to obtain CAB–*C. odorata* core microcapsules.

This step converts biomass-derived phytochemicals into a stable, biodegradable delivery system and represents a scalable, eco-friendly approach to producing bio-based functional materials for subsequent $Zn(OH)_2$ surface modification.

2.4 Surface Coating with Zinc Hydroxide

Surface coating of CAB-based microcapsules with $Zn(OH)_2$ was performed as the final functionalization step in the biomass-to-bioproduct conversion process. The procedure introduced inorganic antibacterial functionality through a mild, aqueous precipitation route consistent with green biorefinery principles.

Dried CAB–*C. odorata* microcapsules (0.5 g) were dispersed in 50 mL of deionized water under stirring at room temperature. Aqueous $Zn(NO_3)_2$ solutions (20–80 mmol/L) were added to control $Zn(OH)_2$ loading. Sodium hydroxide (0.1 M) was added dropwise until pH ≈ 9.5 to initiate in situ precipitation of $Zn(OH)_2$ on the

microcapsule surfaces. The reaction proceeded for 60 min, followed by centrifugation (4,000 rpm, 10 min), triple washing with deionized water, and drying at 40°C for 24 h.

The hybrid samples were labeled CAB–Zn–20, CAB–Zn–40, CAB–Zn–60, and CAB–Zn–80. This eco-safe coating process avoids high temperatures and organic solvents, minimizing energy input and waste generation. The controlled $Zn(OH)_2$ deposition enhances surface activity and antibacterial performance, representing a sustainable hybridization stage within the biomass valorization framework.

2.5 Characterization of Microcapsules

Physicochemical characterization was performed to verify the structural integrity and functional properties of the biomass-derived hybrid microcapsules. Analytical techniques were selected to evaluate each stage of the biorefinery-inspired process, from biomass encapsulation to $Zn(OH)_2$ surface coating. Fourier-transform infrared spectroscopy (FTIR, Bruker Tensor 27) identified functional groups and chemical interactions among *C. odorata* phytochemicals, CAB, and $Zn(OH)_2$ within 4000–400 cm^{-1}. X-ray diffraction (XRD, PANalytical X'Pert PRO, Cu Kα, λ = 1.5406 Å) confirmed crystalline phase formation and $Zn(OH)_2$ incorporation, scanned at 2θ = 10°–80°. Thermogravimetric analysis (TGA, Mettler-Toledo TGA/DSC 1) assessed thermal stability under nitrogen (30–800°C, 10°C min^{-1}), with enhanced stability indicating successful hybridization. Scanning electron microscopy (SEM, Hitachi SU5000) with EDS mapping revealed surface morphology and uniform Zn distribution. Particle size and ζ-potential (Malvern Zetasizer Nano ZS) were measured to evaluate suspension stability. Collectively, these analyses confirm the efficiency of the biomass-to-bioproduct conversion, demonstrating improved material stability and structure–property correlation essential for sustainable antibacterial composites in biorefinery applications.

2.6 Evaluation of antibacterial properties

The antibacterial activity of biomass-derived CAB–$Zn(OH)_2$ hybrid microcapsules was evaluated to verify their performance as sustainable bio-based materials. Tests were conducted against *Escherichia coli* (ATCC 25922) and *Staphylococcus aureus* (ATCC 25923), representing Gram-negative and Gram-positive bacteria relevant to biomedical and environmental applications.

A broth microdilution method following CLSI guidelines was used with slight modification for particulate samples. Bacterial suspensions (≈ 1×10^6 CFU/mL) were exposed to serial dilutions of CAB–Zn–x microcapsules (x = 20–80 mmol/L Zn precursor) at final concentrations of 0.8–25.6 mg/mL in 96-well plates. After incubation at 37°C for 24 h, the minimum inhibitory concentration (MIC) was identified as the lowest concentration preventing visible growth. Minimum bactericidal concentration (MBC) values were confirmed by plating aliquots from growth-inhibited wells on nutrient agar.

All measurements were performed in triplicate, and antibacterial efficiency was expressed as mean MIC and MBC ± SD. The results validated synergistic antibacterial effects between biomass-derived phytochemicals and $Zn(OH)_2$ coating, linking hybrid composition to functional bioactivity. This evaluation confirms the conversion of renewable biomass into eco-efficient antibacterial composites aligned with biorefinery and circular economy principles.

3. Results and Discussion

3.1 Extraction of Chromolaena odorata Leaves and Microcapsule Appearance

The extraction and preparation of *Chromolaena odorata* (Siam weed) leaf extract are illustrated in Fig. 1. Freshly harvested leaves (Fig. 1a) were thoroughly washed, air-dried under ambient conditions (Fig. 1b), and finely chopped to enhance solvent penetration during extraction. Ethanol was selected as the extraction solvent due to its intermediate polarity and effectiveness in solubilizing a wide range of phytochemicals, including flavonoids, alkaloids, tannins, and chlorophyll—compounds known for their antimicrobial and antioxidant activities [13]. After rotary evaporation to remove ethanol, the concentrated extract was freeze-dried to yield a stable dark green powder (Fig. 1c), which was used as the core bioactive agent for microencapsulation. This step demonstrates the valorization of *C. odorata* leaf biomass into extractives containing bioactive phytochemicals, representing a value-added route for invasive plant utilization.

The visual appearance of the resulting microcapsules, prepared using CAB and surface-functionalized with varying concentrations of $Zn(OH)_2$, is shown in Fig. 2. The uncoated microcapsules (CAB-Zn-0; Fig. 2a) exhibited a deep green color, indicating the presence of exposed extract on the particle surface. With increasing $Zn(OH)_2$ precursor concentrations from 10 to 40 mM (Figs. 2b–2e), the microcapsules displayed progressively lighter and more uniform coloration, suggesting enhanced surface coverage by the deposited $Zn(OH)_2$ layer [11].

This change in visual appearance corresponds to structural modifications confirmed by FTIR and SEM analyses (discussed in subsequent sections), which verify successful $Zn(OH)_2$ precipitation and surface coating. The $Zn(OH)_2$ layer serves a dual function: (i) protecting encapsulated phytochemicals from premature degradation [14] and (ii) enabling controlled release of Zn^{2+} ions, which enhance antibacterial efficacy through mechanisms such as membrane disruption and reactive oxygen species (ROS) generation [15].

These findings establish a direct correlation between $Zn(OH)_2$ concentration and microcapsule structural attributes, supporting the formulation's potential as a controlled-release antimicrobial platform for biomedical coatings, wound care, and food-contact materials.

3.2 Characterization of microcapsules

3.2.1 XRD Analysis

X-ray diffraction (XRD) was used to assess the crystalline phases of $Zn(OH)_2$-coated *C. odorata* microcapsules (Fig. 3). Distinct peaks observed in CAB-Zn-10 to CAB-Zn-40 matched orthorhombic $Zn(OH)_2$ (JCPDS No. 01-076-1778), with characteristic reflections at 2θ = 20.09°, 20.81°, 24.98°, 27.11°, 27.65°, and 32.73° [16]. Increasing precursor concentration led to sharper, more intense peaks, indicating progressive crystallization.

CAB-Zn-10 showed broad, low-intensity peaks superimposed on an amorphous background, while CAB-Zn-40 exhibited well-defined diffraction patterns, confirming surface deposition of highly crystalline $Zn(OH)_2$. Enhanced crystallinity correlates with improved Zn^{2+} ion release control and stability—key for antimicrobial efficacy via membrane disruption, ROS generation, and enzyme inhibition [17]. These findings reinforce that higher $Zn(OH)_2$ loading improves both structural integrity and sustained antibacterial performance [18], making CAB-Zn-40 a promising candidate for biomedical and packaging applications.

3.2.2 FTIR Analysis

FTIR spectroscopy was used to investigate molecular interactions between *C. odorata* extract, the CAB matrix, and $Zn(OH)_2$ coating (Fig. 4). The crude extract exhibited a broad O–H stretch at 3317 cm^{-1} and prominent peaks at 1618, 1512, and 1348 cm^{-1}, consistent with phenolic O–H, aromatic C = C, and C–N/C–O vibrations from bioactive phytochemicals [19, 20].

Uncoated microcapsules (CAB-Zn-0) retained key spectral features from both the extract and CAB, including O–H stretching (~ 3400 cm^{-1}) and ester C = O stretching (~ 1700–1600 cm^{-1}), suggesting successful encapsulation and non-covalent interactions [21].

In $Zn(OH)_2$-coated microcapsules (CAB-Zn-40), attenuation of O–H and C = O bands, along with the appearance of Zn–O vibrations at 715 and 545 cm^{-1}, indicate coordination between Zn^{2+} ions and electron-donating groups in the extract [22]. These shifts suggest chemical interaction rather than mere surface adsorption.

Such coordination is expected to enhance Zn^{2+} retention and modulate release kinetics while stabilizing encapsulated actives. This supports a dual-action antimicrobial mechanism: rapid bacteriostasis from phytochemicals and sustained oxidative and enzymatic stress from Zn^{2+} ions—highlighting the system's potential for wound healing, antimicrobial coatings, and active packaging.

3.2.3 EDS Analysis

Energy-dispersive X-ray spectroscopy (EDS) was utilized to evaluate the surface elemental composition of $Zn(OH)_2$-coated *C. odorata* microcapsules. Representative spectra are shown in Fig. 5. Prominent peaks corresponding to carbon (C) and oxygen (O) were detected across all samples, originating from the CAB polymer matrix and plant-derived phytochemicals. The presence of zinc (Zn) in the coated formulations confirmed the successful deposition of $Zn(OH)_2$ onto the microcapsule surfaces.

Minor peaks for gold (Au) and sodium (Na) were also observed. Gold was introduced during the sputter-coating process used for SEM preparation, while sodium likely originated from trace residuals of precursor salts or buffer systems. Importantly, Zn was the only metal with recognized antimicrobial functionality, validating its selective incorporation [23].

Quantitative EDS analysis revealed a clear, concentration-dependent increase in surface Zn content. Both CAB-Zn-10 and CAB-Zn-20 exhibited low zinc content (~ 0.1 wt%), while CAB-Zn-30 and CAB-Zn-40 demonstrated substantially higher Zn loading (~ 0.5 wt%). This trend is consistent with XRD findings and

visually corroborated by SEM observations, indicating that increased precursor concentrations lead to greater $Zn(OH)_2$ accumulation on the microcapsule surface.

The enhanced zinc content in CAB-Zn-30 and CAB-Zn-40 is expected to promote more effective and sustained Zn^{2+} ion release, which contributes to antimicrobial activity through multiple mechanisms. These include disruption of microbial membranes, generation of reactive oxygen species (ROS), and inhibition of bacterial enzyme systems. The ability to tune $Zn(OH)_2$ deposition through precursor concentration offers a valuable design parameter for tailoring antimicrobial efficacy and longevity [24].

Overall, EDS analysis confirms the uniform and controllable surface functionalization of the microcapsules, supporting the reliability of the fabrication method. These results reinforce the functional role of $Zn(OH)_2$ in enhancing microcapsule performance, highlighting the potential of CAB-Zn-40 as a scalable and adaptable antimicrobial platform for biomedical, pharmaceutical, and environmental applications.

3.2.4 SEM Analysis

Scanning electron microscopy (SEM) was employed to examine the surface morphology of *C. odorata*-loaded CAB microcapsules coated with increasing concentrations of $Zn(OH)_2$ (Fig. 6). The uncoated control (CAB-Zn-0) exhibited smooth, spherical surfaces, reflecting the uniformity of the CAB matrix and the absence of surface-bound inorganic phases.

At 10 mM $Zn(OH)_2$ (CAB-Zn-10), mild surface roughening and discrete nanoparticle aggregates were observed, indicating initial $Zn(OH)_2$ nucleation. Increasing the concentration to 20 mM (CAB-Zn-20) led to more continuous and heterogeneous surface coverage, enhancing surface area and potentially facilitating improved Zn^{2+} ion diffusion for antibacterial activity [25, 26].

At 30 mM (CAB-Zn-30), a denser and more compact coating formed, with aggregated nanoparticle domains promoting prolonged Zn^{2+} release and microbial contact. The 40 mM sample (CAB-Zn-40) demonstrated the most extensive and uniform nanoparticle coverage, characterized by a highly textured, near-saturated $Zn(OH)_2$ layer—providing an optimal interface for sustained ion release, ROS generation, and inhibition of bacterial adhesion or biofilm formation [27].

These findings highlight a clear, concentration-dependent morphological evolution. The nanostructured coatings in CAB-Zn-30 and CAB-Zn-40 offer enhanced surface functionality and sustained antimicrobial potential, underscoring their suitability for biomedical and environmental applications.

3.2.5 Particle size distribution Analysis

Figure 7 and Table 1 illustrate the particle size distribution of *C. odorata*-loaded CAB microcapsules coated with increasing concentrations of $Zn(OH)_2$. A consistent increase in mean diameter was observed with higher precursor concentrations, confirming progressive $Zn(OH)_2$ deposition. Uncoated microcapsules (CAB-Zn-0) averaged 1013.3 ± 66.5 nm, increasing modestly with 10 mM $Zn(OH)_2$ (1049.5 ± 74.5 nm) and reaching 1275.3 ± 109.9 nm at 40 mM (CAB-Zn-40).

This size enlargement reflects the formation of thicker $Zn(OH)_2$ shells, which enhance Zn^{2+} reservoir capacity and enable sustained, diffusion-controlled ion release. The denser coatings also reduce premature Zn^{2+} leaching, promoting prolonged antimicrobial activity [28]. Additionally, increased particle size and surface roughness may hinder bacterial adhesion, offering synergistic physical–chemical antibacterial effects. CAB-Zn-40, with the largest and most uniform particles, is thus well-suited for durable applications such as wound dressings, antimicrobial coatings, and controlled-release systems.

Table 1
Particle size and thermal degradation characteristics of CAB–$Zn(OH)_2$ microcapsules prepared with different Zn precursor concentrations. Increasing $Zn(OH)_2$ loading led to larger particle sizes and improved thermal stability, indicating the formation of thicker inorganic coatings and enhanced structural integrity of the hybrid microcapsules.

Sample	Mean Particle Size (nm)	Initial Onset Temperature (°C)	Final Onset Temperature (°C)	Weight Loss (%)
CAB–Zn–0	1013.3 ± 66.5	336.7	385.3	85.90
CAB–Zn–10	1049.5 ± 74.5	252.6	368.8	48.94
CAB–Zn–20	1159.8 ± 58.8	292.8	371.2	37.57
CAB–Zn–30	1202.5 ± 82.8	274.4	371.3	28.33
CAB–Zn–40	1275.3 ± 109.9	287.0	367.8	28.05

3.2.6 TGA Analysis

Thermogravimetric analysis (Fig. 8, Table 1) revealed the thermal degradation behavior of *C. odorata*-loaded CAB microcapsules across varying $Zn(OH)_2$ coating levels. All samples showed primary mass loss between 250–400°C, attributed to degradation of the CAB matrix and embedded phytochemicals. Uncoated microcapsules (CAB-Zn-0) exhibited the highest weight loss (85.90%) and an onset degradation temperature of 336.7°C, indicating low thermal resistance.

$Zn(OH)_2$-coated samples showed progressively enhanced thermal stability. Despite a slightly lower onset temperature in CAB-Zn-10 (252.6°C), its reduced weight loss (48.94%) suggests partial stabilization. Further increases in $Zn(OH)_2$ content led to lower total weight losses: 37.57% (CAB-Zn-20), 28.33% (CAB-Zn-30), and 28.05% (CAB-Zn-40), with CAB-Zn-40 also exhibiting a higher onset temperature (287.0°C).

These improvements are attributed to the $Zn(OH)_2$ coating, which acts as a thermal and oxidative barrier, limiting volatilization of thermolabile components and enhancing structural integrity [29]. Enhanced thermal resistance supports product longevity and functionality under elevated temperatures—critical for applications such as antimicrobial wound dressings, medical textiles, and heat-resistant packaging—where retention of bioactivity and controlled Zn^{2+} release are essential.

The enhanced crystallinity and stability indicate that the biopolymer–inorganic hybridization route can upgrade raw biomass into advanced functional materials suitable for bio-based industries.

3.3 Antibacterial Activity

The antibacterial efficacy of *C. odorata*-loaded CAB microcapsules with increasing $Zn(OH)_2$ coating concentrations was assessed against *Escherichia coli* (Gram-negative) and *Staphylococcus aureus* (Gram-positive) via MIC and MBC assays. Results demonstrated a clear concentration-dependent enhancement in antibacterial performance, particularly against the more resilient *E. coli*, highlighting the synergistic roles of phytochemicals, sustained Zn^{2+} release, and ROS generation.

3.3.1 Minimum Inhibitory Concentration (MIC)

MIC values (Fig. 9) decreased significantly with higher $Zn(OH)_2$ content. CAB-Zn-40 exhibited the strongest inhibition, with MICs of 12.8 mg/mL for *E. coli* and 6.4 mg/mL for *S. aureus*. While lower $Zn(OH)_2$ coatings (CAB-Zn-10, CAB-Zn-20) retained activity against *S. aureus*, they were less effective against *E. coli*, reflecting differences in cell wall permeability. Enhanced Zn^{2+} release and ROS-mediated damage likely account for the increased efficacy in higher-coated systems.

3.3.2 Minimum Bactericidal Concentration (MBC)

MBC data (Table 2, Figs. 9–10) closely followed MIC trends. CAB-Zn-40 demonstrated complete bactericidal activity at 12.8 µg/mL against *E. coli* and 6.4 µg/mL against *S. aureus*, surpassing the performance of lower $Zn(OH)_2$-coated formulations, which required concentrations of 25.6 µg/mL or higher. This enhanced potency is attributed to a combination of mechanisms: disruption of bacterial membranes through Zn^{2+} interactions with cell wall components, oxidative damage induced by reactive oxygen species (ROS) targeting lipids, proteins, and nucleic acids, and interference with intracellular processes, including enzymatic inhibition and transcriptional disruption [30].

In contrast to uncoated microcapsules that rely solely on phytochemical activity, $Zn(OH)_2$-coated systems provide a sustained, multi-mechanistic antibacterial response. CAB-Zn-40, in particular, demonstrates superior efficacy along with improved thermal stability, controlled Zn^{2+} release, and minimized cytotoxicity risk, making it a compelling candidate for applications requiring long-term antimicrobial performance, such as wound dressings, infection-resistant coatings, and bioactive packaging [31].

Table 2
Minimum bactericidal concentration (MBC) values of CAB microcapsules against *E. coli* and *S. aureus*. The CAB-Zn-40 formulation exhibits the lowest MBCs, reflecting synergistic bactericidal effects from phytochemicals and Zn^{2+} ion release.

Microcapsule Type	MBC (*E. coli*) (µg/mL)	MBC (*S. aureus*) (µg/mL)
CAB-Zn-0	25.6	25.6
CAB-Zn-10	51.2	51.2
CAB-Zn-20	51.2	25.6
CAB-Zn-30	25.6	12.8
CAB-Zn-40	12.8	6.4

The strong performance of CAB–Zn–40 underscores the potential of biomass-derived formulations as sustainable substitutes for synthetic antimicrobial plastics.

3.4 Mechanistic Insight into Antibacterial Activity

The superior antibacterial efficacy of $Zn(OH)_2$-coated *Chromolaena odorata* microcapsules—particularly the CAB-Zn-40 formulation—is attributed to a synergistic set of mechanisms operating at both the surface and intracellular levels (Fig. 11). These include sustained Zn^{2+} ion release, generation of reactive oxygen species (ROS), bacterial membrane disruption, and metabolic interference. Collectively, these effects contribute to potent and prolonged bactericidal activity.

3.4.1 Zn^{2+}-Mediated ROS Generation and Oxidative Stress

A key antibacterial mechanism involves the sustained release of Zn^{2+} ions from the $Zn(OH)_2$-coated microcapsule surface. SEM and EDS analyses confirmed that Zn surface content increases with precursor concentration, facilitating controlled and prolonged ion diffusion into the surrounding medium. Once released, Zn^{2+} ions catalyze intracellular redox reactions, generating reactive oxygen species (ROS) including superoxide anions (O_2^-), hydrogen peroxide (H_2O_2), and hydroxyl radicals (•OH) [32, 33].

These ROS species exert oxidative stress by targeting bacterial lipids, proteins, and nucleic acids, ultimately leading to cell dysfunction and death. The high crystallinity of $Zn(OH)_2$—particularly evident in CAB-Zn-40 as revealed by XRD—further supports its role in enabling sustained Zn^{2+} release and consistent ROS generation. These results suggest that $Zn(OH)_2$ coatings function analogously to ZnO systems, delivering continuous antibacterial action through dual chemical pathways, and thus play a central role in the long-term efficacy of the coated microcapsules.

3.4.2 Bacterial Membrane Disruption

SEM analysis revealed a marked increase in surface roughness with higher $Zn(OH)_2$ loading, particularly in CAB-Zn-30 and CAB-Zn-40. These nanostructured coatings enhance contact with bacterial membranes,

intensifying localized Zn^{2+} ion release and promoting ROS-induced lipid peroxidation. This behavior is consistent with previous findings on Cu^{2+} systems reported by Pookmanee et al. (2025) [34].

The resulting membrane damage leads to the leakage of intracellular contents, cytoplasmic collapse, and eventual cell lysis [35]. The synergistic interplay between chemical factors (Zn^{2+} ions and ROS) and physical effects (surface roughness and nanoparticle intrusion) accelerates membrane destabilization. This dual-action mechanism underpins the significantly reduced MIC and MBC values observed in higher $Zn(OH)_2$-coated formulations, confirming their potent and irreversible antibacterial activity.

3.4.3 Cellular Dysfunction and Stress Response

Beyond membrane-level interactions, Zn^{2+} ions interfere with vital intracellular processes. By binding to enzymatic cofactors, Zn^{2+} inhibits key metabolic enzymes, disrupts ribosomal function, and impairs DNA replication. Accumulated ROS further aggravates cellular stress, potentially inducing defense responses such as oxidative stress gene expression and DNA repair mechanisms [36].

Although these molecular responses were not directly evaluated in this study, future transcriptomic or proteomic analyses could provide insight into bacterial adaptation and resistance pathways triggered by $Zn(OH)_2$ exposure.

3.4.4 Synergistic Antimicrobial Mechanism

The antibacterial effect of CAB-Zn-40 is not solely due to $Zn(OH)_2$ but also enhanced by bioactive phytochemicals from *C. odorata*. Compounds such as flavonoids, tannins, and alkaloids are known to destabilize membranes and inhibit metabolic enzymes [37, 38]. The $Zn(OH)_2$ coating amplifies this effect by enabling sustained Zn^{2+} release and ROS production, resulting in a dual-action antimicrobial system.

Additional support is provided by TGA and DLS data, which indicate improved structural stability and encapsulation efficiency at higher $Zn(OH)_2$ concentrations. These attributes ensure functional retention under environmental or physiological stress and contribute to long-term antimicrobial performance.

Together, these mechanistic insights highlight CAB-Zn-40 as a multifunctional antimicrobial platform. By integrating phytochemical bioactivity with sustained-release nanocoating, this system offers a promising strategy for applications requiring prolonged antibacterial efficacy, including wound care, bioactive medical coatings, and antimicrobial packaging materials.

3.5 Comparative Antibacterial Activity Against Staphylococcus aureus and Escherichia coli

To contextualize the antibacterial efficacy of the $Zn(OH)_2$-coated *Chromolaena odorata* microcapsules developed in this study, a comparative analysis was conducted using literature-reported plant-based antimicrobial systems (Table 3). These systems include uncoated plant extracts, polymer-encapsulated phytochemicals, and metal-functionalized microcapsules.

Early studies utilizing *C. odorata* ethanolic extracts [39] or isolated flavonoids [40] demonstrated strong in vitro antibacterial activity, with MIC values ranging from 0.016 to 6.25 mg/mL. However, these formulations suffer from critical limitations—namely, rapid chemical degradation, poor thermal stability, and lack of sustained antimicrobial release—reducing their practical utility in long-term applications.

To address these issues, microencapsulation has emerged as a viable strategy. For example, Liu et al. (2023) [41] reported the encapsulation of cinnamon essential oil in gum arabic/maltodextrin microcapsules, which improved chemical stability and demonstrated moderate antibacterial activity. However, such systems—lacking an inorganic phase—are often limited in durability and spectrum of action under physiologically relevant conditions.

In more recent approaches, the integration of antimicrobial metals has shown considerable promise. Li et al. (2023) [42] developed silver nanoparticle (AgNP)-coated chitosan–gelatin microcapsules containing *Ginkgo biloba* essential oil, while Sharma et al. (2024) [43] formulated ZnO-coated chitosan–cellulose microcapsules loaded with *Plumeria obtusa* extract. These systems leveraged metal ion release to enhance bactericidal activity; however, they often lacked quantitative MIC data or comprehensive benchmarking against plant–metal hybrid systems. In contrast, the CAB-Zn-40 formulation presented in this study uniquely combines plant-derived bioactive compounds, a biodegradable CAB matrix, and a $Zn(OH)_2$ nanocoating that enables sustained Zn^{2+} release and reactive oxygen species (ROS) generation, along with demonstrated thermal stability confirmed by TGA analysis.

This formulation achieved MIC values of 12.8 mg/mL against *E. coli* and 6.4 mg/mL against *S. aureus*, outperforming several uncoated extract-based systems and rivaling metal-functionalized designs. Additionally, its high crystallinity, structural integrity, and dual-mode antibacterial action position it as a promising candidate for applications requiring both efficacy and durability—such as wound care, biomedical coatings, and active packaging.

Table 3
Comparative summary of antimicrobial plant-based microcapsule systems reported in the literature. The CAB-Zn-40 formulation demonstrates favorable performance and stability relative to uncoated and metal-integrated formulations.

Plant Extract	Encapsulation Material	Metal Component	Controlled Release	Stability	*Antibacterial Effectiveness (MIC)**	Reference
C. odorata (ethanol extract)	None	None	No	Low (rapid degradation)	6.25 mg/mL (*E. coli*), 3.125 mg/mL (*S. aureus*)	[39]
Isolated *C. odorata* flavonoids	None	None	No	Low	0.016–0.031 mg/mL (*both strains*)	[40]
Cinnamon essential oil	Gum arabic / Maltodextrin	None	Yes (EO release)	High	14 µL/mL (*E. coli*), 7 µL/mL (*S. aureus*)	[41]
Ginkgo biloba EO	Chitosan–gelatin	AgNPs	Yes (Ag^+, EO release)	High (spray-dried)	Not reported (inhibition zones confirmed)	[42]
Plumeria obtusa leaf extract	Chitosan–cellulose	ZnO nanoparticles	Yes (Zn^{2+} release)	Structurally stable	Not reported (qualitative activity)	[43]
C. odorata extract	Cellulose acetate butyrate (CAB)	$Zn(OH)_2$ coating	Yes (Zn^{2+} release)	High (TGA confirmed)	12.8 mg/mL (*E. coli*), 6.4 mg/mL (*S. aureus*)	This study (CAB-Zn-40)

* MIC values are reported as published; due to variation in test protocols, results are indicative and not directly comparable.

4. Conclusions

This study demonstrates a green valorization pathway for transforming *Chromolaena odorata* biomass into high-value antibacterial materials within the framework of sustainable biorefinery. A biodegradable cellulose acetate butyrate (CAB) matrix, derived from renewable cellulose resources, was successfully integrated with plant-extracted phytochemicals and coated with zinc hydroxide ($Zn(OH)_2$) via an eco-friendly in situ precipitation process. This mild, solvent-minimized route represents an environmentally responsible conversion process that utilizes invasive plant biomass as a renewable feedstock rather than a waste resource.

The resulting CAB–$Zn(OH)_2$ hybrid microcapsules exhibited enhanced crystallinity, thermal stability, and surface functionality, confirming successful hybridization between the bio-based polymer and inorganic coating. Among the formulations, CAB–Zn–40 displayed the strongest antibacterial performance against

Escherichia coli and *Staphylococcus aureus*, attributed to the synergistic effects of sustained Zn^{2+} release and plant-derived bioactive compounds. This combination produced a durable, controlled-release antibacterial response suitable for biomedical and packaging applications.

Beyond material performance, the work highlights a scalable example of biomass-to-bioproduct conversion that aligns with circular bioeconomy principles. The valorization of *C. odorata*, an invasive tropical species, into a biodegradable antibacterial platform demonstrates how underutilized biomass can be transformed into eco-efficient, high-value functional materials. Future research will focus on evaluating biodegradation kinetics, environmental life-cycle performance, and techno-economic feasibility to further integrate this approach into sustainable biorefinery systems.

Declarations

Ethical Approval

Not applicable.

Consent for publication

Not applicable.

Competing interest

The authors declare no conflicts of interest, whether personal relationships or financial considerations, that could have influenced the publication of this study.

Funding

No funding was received to assist with the preparation of this manuscript.

Author Contribution

J.K. supervised the study and contributed to conceptualization, methodology, and writing (original draft, review, and editing). M.B. and S.Y. contributed to methodology, investigation, validation. P.K. contributed to methodology, investigation, validation. P.U. performed investigation and validation. P.J. led conceptualization, methodology, writing (original draft, review, and editing). All authors reviewed and approved the final manuscript.

Acknowledgement

We sincerely appreciate the generous support provided by the Thailand Scientific Research and Innovation (TSRI) for this study.

Data Availability

The data are available from the corresponding author upon reasonable request.

References

1. Ferdinand AS, Coppo MJ, Howden BP, Browning GF (2023) Tackling antimicrobial resistance by integrating One Health and the Sustainable Development Goals. BMC Glob Public Health 1:11. https://doi.org/10.1186/s44263-023-00003-8
2. Angelini P (2024) Plant-derived antimicrobials and their crucial role in combating antimicrobial resistance. Antibiotics 13:746. https://doi.org/10.3390/antibiotics13080746
3. Jubair N, Rajagopal M, Chinnappan S, Abdullah NB, Fatima A (2021) Review on the antibacterial mechanism of plant-derived compounds against multidrug-resistant bacteria (MDR). Evid Based Complement Alternat Med 2021:3663315. https://doi.org/10.1155/2021/3663315
4. Olawale F, Olofinsan K, Iwaloye O (2022) Biological activities of *Chromolaena odorata*: A mechanistic review. S Afr J Bot 144:44–57. https://doi.org/10.1016/j.sajb.2021.09.001
5. Yanis MA, Amirsyah M, Harsono AD (2024) Healing potential of *Chromolaena odorata* extract: Modulation of neutrophil, macrophage, and lymphocyte response in infected wounds of *Mus musculus*. J Penelit Pendidik IPA 10:10670–10676. https://doi.org/10.29303/jppipa.v10i12.9423
6. Pérez-Pérez V, Jiménez-Martínez C, González-Escobar JL, Corzo-Ríos LJ (2024) Exploring the impact of encapsulation on the stability and bioactivity of peptides extracted from botanical sources: trends and opportunities. Front Chem 12:1423500. https://doi.org/10.3389/fchem.2024.1423500
7. Rezagholizade-Shirvan A, Soltani M, Shokri S, Radfar R, Arab M, Shamloo E (2024) Bioactive compound encapsulation: Characteristics, applications in food systems, and implications for human health. Food Chem X 24:101953. https://doi.org/10.1016/j.fochx.2024.101953
8. Emon DD, Islam MS, Mazumder MAR, Aziz MG, Rahman MS (2025) Recent applications of microencapsulation techniques for delivery of functional ingredients in food products: A comprehensive review. Food Chem Adv 6:100923. https://doi.org/10.1016/j.focha.2025.100923
9. Silva MV, Serge-Correales YE, Pereira LH, da Barud S, Ribeiro H, Otaguro SJ, Assunção H RMD (2025) Cellulose acetate butyrate films as a platform for energy upconversion composites: Design and properties. ACS Omega 10:18125–18134. https://doi.org/10.1021/acsomega.5c02294
10. Mendes CR, Dilarri G, Forsan CF, Sapata VDMR, Lopes PRM, de Moraes PB, Montagnolli RN, Ferreira H, Bidoia ED (2022) Antibacterial action and target mechanisms of zinc oxide nanoparticles against bacterial pathogens. Sci Rep 12:2658. https://doi.org/10.1038/s41598-022-06617-2
11. Srivastava M, Singh KR, Singh T, Asiri M, Suliman M, Sabia H, Deen PR, Chaube R, Singh J (2023) Bioinspired fabrication of zinc hydroxide-based nanostructure from lignocellulosic biomass *Litchi chinensis* leaves and its efficacy evaluation on antibacterial, antioxidant, and anticancer activity. Int J Biol Macromol 253:126886. https://doi.org/10.1016/j.ijbiomac.2023.126886
12. Ketwaraporn J, Pinthong S, Kerdphu R, Daebau S, Kraivuttinun P, Jansanthea P (2024) Microencapsulation of *Chromolaena odorata* leaf extract with cellulose esters for the application as an

eco-friendly antibacterial agent. Indones J Chem 24:1527–1540. https://doi.org/10.22146/ijc.95841

13. Kumar A, P N, Kumar M, Jose A, Tomer V, Oz E, Proestos C, Zeng M, Elobeid T, Sneha K, Oz F (2023) Major phytochemicals: recent advances in health benefits and extraction methods. Molecules 28:887. https://doi.org/10.3390/molecules28020887
14. Lobel BT, Baiocco D, Al-Sharabi M, Routh AF, Zhang Z, Cayre OJ (2024) Current challenges in microcapsule designs and microencapsulation processes: a review. ACS Appl Mater Interfaces 16:40326–40355. https://doi.org/10.1021/acsami.4c02462
15. Afrasiabi S, Saghatchi F, Dehpour AR, Goudarzi R, Karimi MR, Partoazar A (2025) Biocompatibility and photoinactivation evaluation of zinc hydroxide chloride nanosheets against *Streptococcus mutans*. BMC Microbiol 25:116. https://doi.org/10.1186/s12866-025-03822-x
16. Gordeeva A, Hsu YJ, Jenei IZ, Carvalho PHB, Simak SI, Andersson O, Häussermann U (2020) Layered zinc hydroxide dihydrate, $Zn_5(OH)_{10}{\cdot}2H_2O$, from hydrothermal conversion of ε-$Zn(OH)_2$ at gigapascal pressures and its transformation to nanocrystalline ZnO. ACS Omega 5:17617–17627. https://doi.org/10.1021/acsomega.0c02075
17. Wei Y, Wang J, Wu S, Zhou R, Zhang K, Zhang Z, Liu J, Qin S, Shi J (2022) Nanomaterial-based zinc ion interference therapy to combat bacterial infections. Front Immunol 13:899992. https://doi.org/10.3389/fimmu.2022.899992
18. Haque S, Faidah H, Ashgar SS, Abujamel TS, Mokhtar JA, Almuhayawi MS, Harakeh S, Singh R, Srivastava N, Gupta VK (2022) Green synthesis of $Zn(OH)_2$/ZnO-based bionanocomposite using pomegranate peels and its application in the degradation of bacterial biofilm. Nanomaterials 12:3458. https://doi.org/10.3390/nano12193458
19. Agatonovic-Kustrin S, Gegechkori V, Petrovich DS, Ilinichna KT, Morton DW (2021) HPTLC and FTIR fingerprinting of olive leaves extracts and ATR-FTIR characterisation of major flavonoids and polyphenolics. Molecules 26:6892. https://doi.org/10.3390/molecules26226892
20. Aldahasi RM, Shami A, Mohammed AE (2024) Bimetallic nanoparticles and biochar produced by *Adansonia digitata* shell and their effect against tomato pathogenic fungi. PeerJ 12:e17023. https://doi.org/10.7717/peerj.17023
21. Seke F, Adiamo OQ, Sultanbawa Y, Sivakumar D (2023) *In vitro* antioxidant activity, bioaccessibility, and thermal stability of encapsulated strawberry fruit (*Fragaria × ananassa*) polyphenols. Foods 12:4045. https://doi.org/10.3390/foods12214045
22. Faheem M, Siddiqi HM, Habib A, Shahid M, Afzal A (2022) ZnO/$Zn(OH)_2$ nanoparticles and self-cleaning coatings for the photocatalytic degradation of organic pollutants. Front Environ Sci 10:965925. https://doi.org/10.3389/fenvs.2022.965925
23. Turner RJ (2024) The good, the bad, and the ugly of metals as antimicrobials. Biometals 37:545–559. https://doi.org/10.1007/s10534-023-00565-y
24. Sahoo J, Sarkhel S, Mukherjee N, Jaiswal A (2022) Nanomaterial-based antimicrobial coating for biomedical implants: new age solution for biofilm-associated infections. ACS Omega 7:45962–45980. https://doi.org/10.1021/acsomega.2c06211
25. Li C, Yun T, Pan G, Tao Y, Lu J, Du J, Wang H (2023) Tailoring flower-like $Zn(OH)_2$ nanoarchitectures and stearic acid on cellulosic fibers for structurally robust superhydrophobic surface. Ind Crops Prod

205:117576. https://doi.org/10.1016/j.indcrop.2023.117576

26. Xiang E, Moran CS, Ivanovski S, Abdal-Hay A (2023) Nanosurface texturing for enhancing the antibacterial effect of biodegradable metal zinc: surface modifications. Nanomaterials 13:2022. https://doi.org/10.3390/nano13132022
27. Malhotra A, Chauhan SR, Rahaman M, Tripathi R, Khanuja M, Chauhan A (2023) Phyto-assisted synthesis of zinc oxide nanoparticles for developing antibiofilm surface coatings on central venous catheters. Front Chem 11:1138333. https://doi.org/10.3389/fchem.2023.1138333
28. Selmani A, Zeiringer S, Šarić A, Stanković A, Učakar A, Vidmar J, Abram A, Džakula BN, Kontrec J, Zore A, Bohinc K, Roblegg E, Matijaković Mlinarić N (2025) ZnO nanoparticle-infused vaterite coatings: A novel approach for antimicrobial titanium implant surfaces. J Funct Biomater 16:108. https://doi.org/10.3390/jfb16030108
29. Ruiz CV, Becerra ME, Giraldo O (2020) Structural, thermal, and release properties of hybrid materials based on layered zinc hydroxide and caffeic acid. Nanomaterials 10:163. https://doi.org/10.3390/nano10010163
30. Ghaffari SB, Sarrafzadeh MH, Salami M, Alvandi A (2024) A comparative study of the action mechanisms and development strategies of different ZnO-based nanostructures in antibacterial and anticancer applications. J Drug Deliv Sci Technol 91:105221. https://doi.org/10.1016/j.jddst.2023.105221
31. Pino P, Bosco F, Mollea C, Onida B (2023) Antimicrobial nano-zinc oxide biocomposites for wound healing applications: a review. Pharmaceutics 15:970. https://doi.org/10.3390/pharmaceutics15030970
32. Sá AS, de Lima IS, Honório LM, Furtini MB, de Souza JKD, dos Santos FEP, Barreto HM, Tabuti TG, da Silva-Filho EC, Triboni ER, Osajima JA (2022) ROS-mediated antibacterial response of ZnO and ZnO containing cerium under light. Chem Pap 76:7051–7060. https://doi.org/10.1007/s11696-022-02390-y
33. Tsuneo I (2022) Anti-bacterial mechanism for metallic Ag^{+}, Cu^{2+}, Zn^{2+} ions-induced bacteriolysis on disruptive OM Lpp and PGN inhibitive elongations against *S. aureus* and *E. coli*. Mathews J Cytol Histol 6:1–13. https://doi.org/10.30654/MJCH.10018
34. Pookmanee P, Khongyot W, Tapala W, Kunthadee P, Puntharod R, Satienperakul S, Kitikul J, Thanomwat M, Chaiwoot P, Phisalayon S, Kuimalee S, Laorodphan N, Niamsup P, Jansanthea P, Ubolsook P, Pookmanee T (2025) Green hydrothermal synthesis of dual-phase submicron Cu_2O–CuO particles using corn husk extract for enhanced antibacterial applications. ChemistrySelect 10:e02184. https://doi.org/10.1002/slct.202502184
35. Krishnamoorthy R, Athinarayanan J, Periyasamy VS, Alshuniaber MA, Alshammari G, Hakeem MJ, Ahmed MA, Alshatwi AA (2022) Antibacterial mechanisms of zinc oxide nanoparticles against bacterial food pathogens resistant to β-lactam antibiotics. Molecules 27:2489. https://doi.org/10.3390/molecules27082489
36. Lin Z, Zhang L, Li D (2024) Interpret the potential role of zinc against oxidative stress in inflammation with a practical fluorescent assay. Bioorg Chem 153:107886. https://doi.org/10.1016/j.bioorg.2024.107886
37. Hridhya KV, Kulandhaivel M (2017) Antimicrobial activity of *Chromolaena odorata* against selected pyogenic pathogens. Int J Pharmacogn Phytochem Res 9:1001–1007. https://doi.org/10.25258/phyto.v9i07.11171

38. Budha Magar A, Shrestha D, Pakka S, Sharma KR (2023) Phytochemistry, biological, and toxicity study on aqueous and methanol extracts of *Chromolaena odorata*. Sci World J 2023:6689271. https://doi.org/10.1155/2023/6689271
39. Ugochi UJ, Obinna AC, Emeka EA, Oluchi AE, Makeri D, Theophilus P, Agwu E (2025) Therapeutic potential of *Chromolaena odorata*, *Vernonia amygdalina*, and *Cymbopogon citratus* against pathogenic bacteria. Sci Rep 15:217. https://doi.org/10.1038/s41598-024-84696-3
40. Omokhua-Uyi AG, Abdalla MA, Leonard CM, Aro A, Uyi OO, Van Staden J, McGaw LJ (2020) Flavonoids isolated from the South African weed *Chromolaena odorata* (Asteraceae) have pharmacological activity against uropathogens. BMC Complement Med Ther 20:15. https://doi.org/10.1186/s12906-020-03024-0
41. Liu H, Zhao Z, Xu W, Cheng M, Chen Y, Xun M, Liu Q, Wang W (2023) Preparation, characterization, release and antibacterial properties of cinnamon essential oil microcapsules. Coatings 13:973. https://doi.org/10.3390/coatings13060973
42. Li L, Lu Y, Chen Y, Bian J, Wang L, Li L (2023) Antibacterial chitosan–gelatin microcapsules modified with green-synthesized silver nanoparticles for food packaging. J Renew Mater 11:1. https://doi.org/10.32604/jrm.2022.021456
43. Sharma B, Upadhyaya D, Deshmukh P, Chakraborty S, Sahu K, Satapathy S, Majumder SK (2024) *Azadirachta indica* (AI) leaf extract coated ZnO–AI nanocore–shell particles for enhanced antibacterial activity against methicillin-resistant *Staphylococcus aureus* (MRSA). Biomed Mater 19:025014. https://doi.org/10.1088/1748-605X/ad1df7

Figures

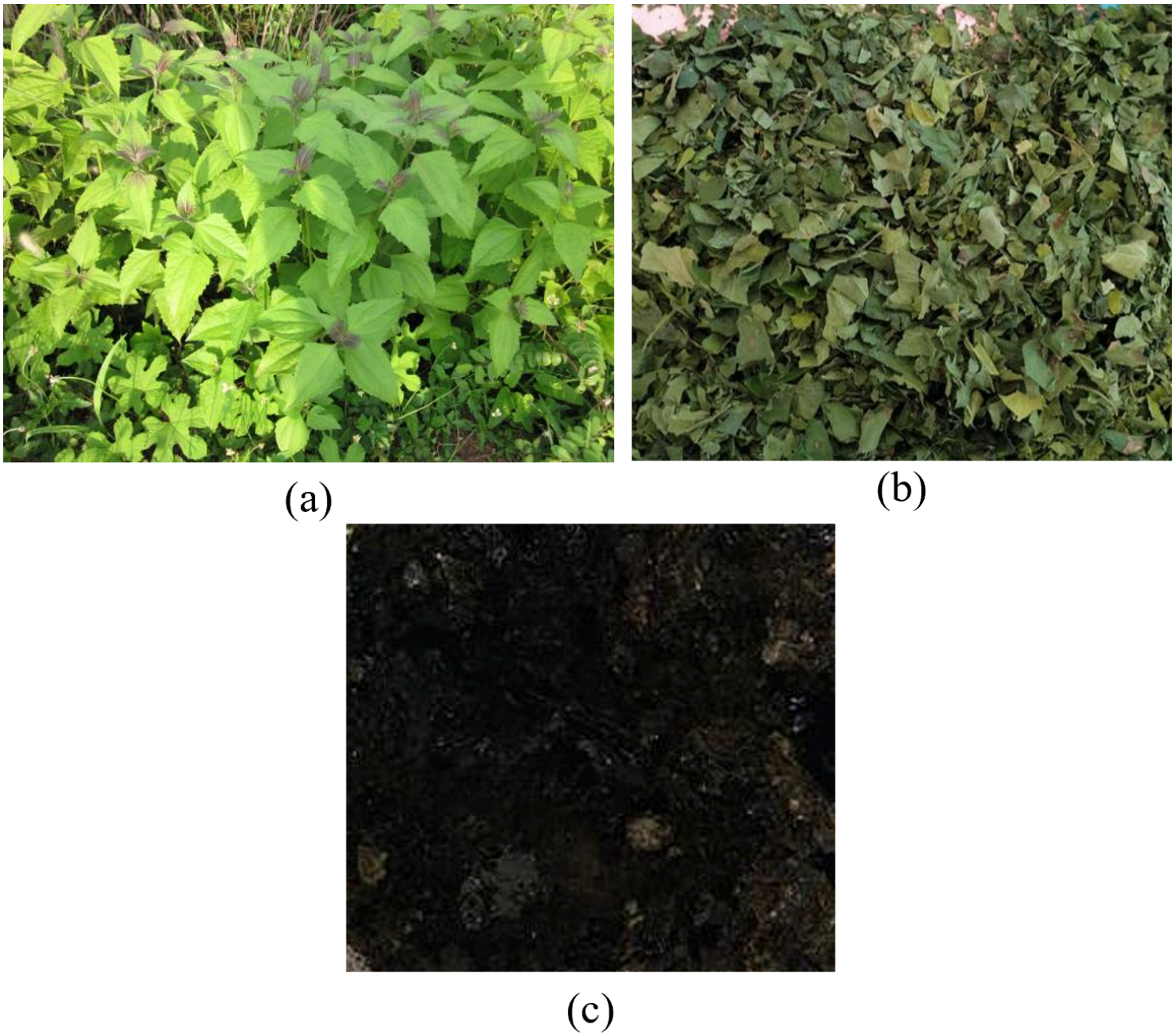

Figure 1

Stepwise preparation of *Chromolaena odorata* extract: (a) freshly harvested leaves, (b) air-dried and chopped material for extraction, and (c) freeze-dried ethanol extract used as the core antimicrobial agent. The process preserves phytochemical integrity and improves storage stability.

Figure 2

Visual appearance of CAB microcapsules coated with increasing concentrations of $Zn(OH)_2$: (a) CAB-Zn-0, (b) CAB-Zn-10, (c) CAB-Zn-20, (d) CAB-Zn-30, and (e) CAB-Zn-40. The progressive shift in color reflects increasing surface deposition of $Zn(OH)_2$.

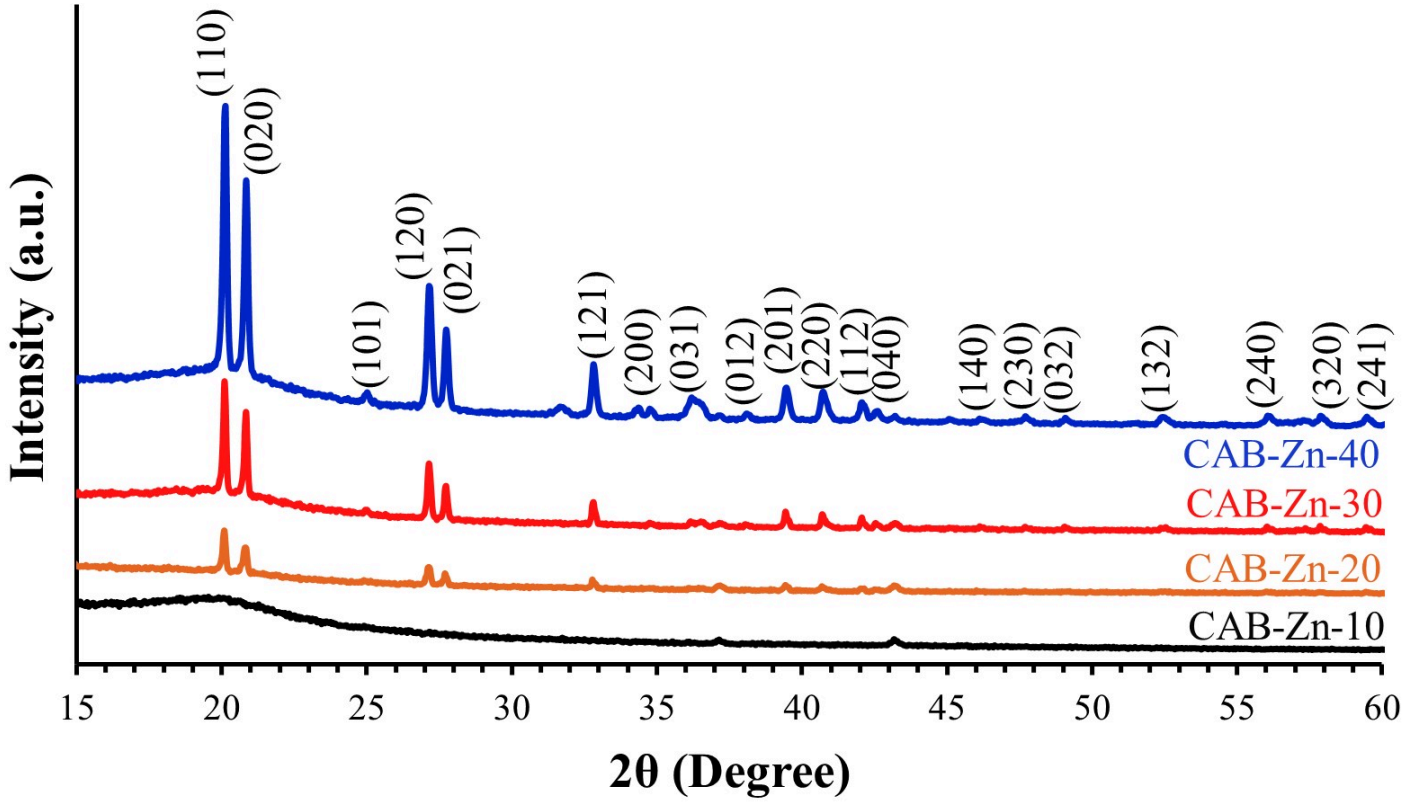

Figure 3

XRD patterns of CAB microcapsules coated with increasing concentrations of $Zn(OH)_2$. The progressive emergence and intensification of diffraction peaks confirm successful surface deposition and enhanced crystallinity of orthorhombic $Zn(OH)_2$ nanostructures.

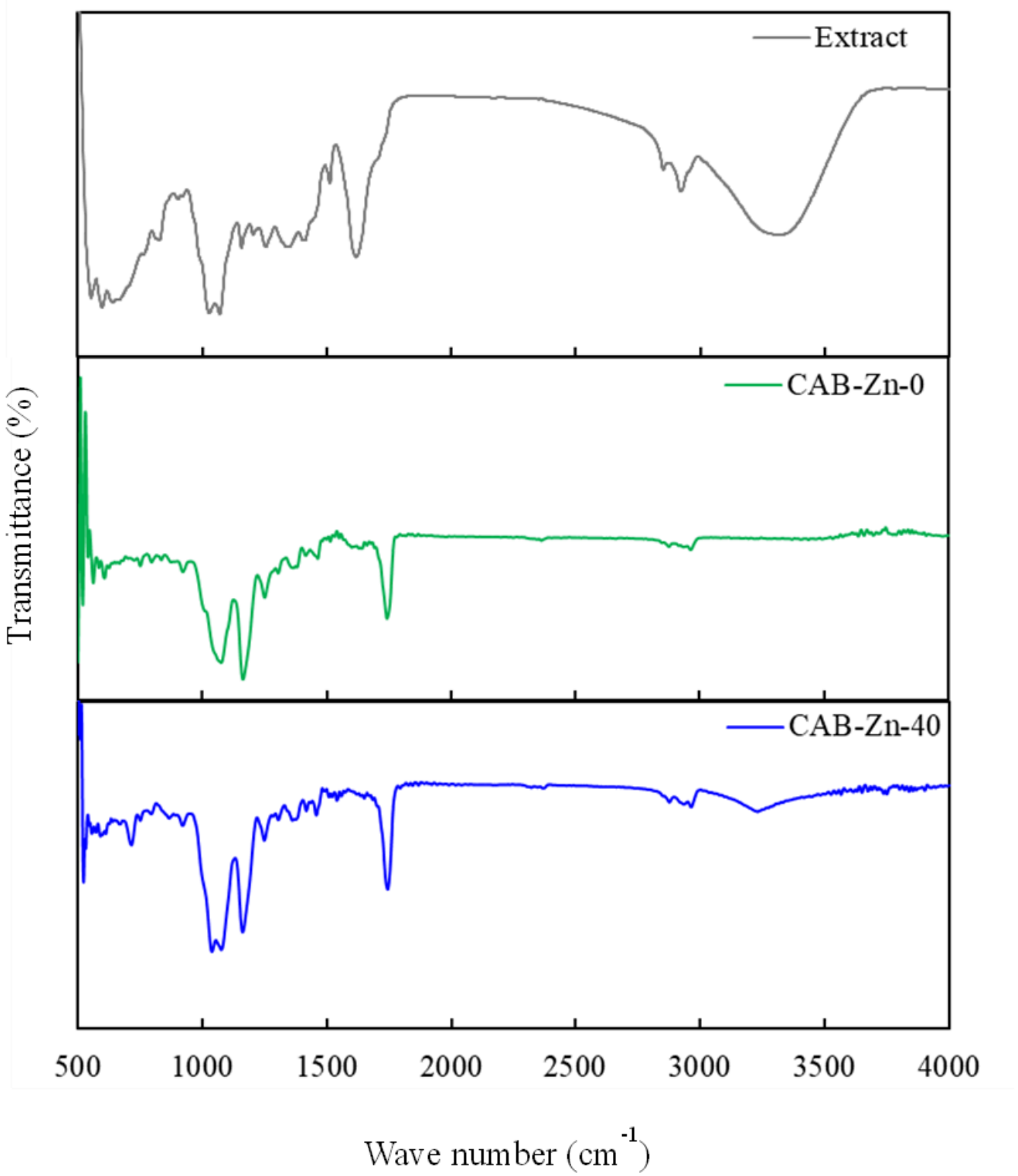

Figure 4

FTIR spectra of (a) crude *C. odorata* extract, (b) uncoated microcapsules (CAB-Zn-0), and (c) $Zn(OH)_2$-coated microcapsules (CAB-Zn-40). Spectral changes highlight Zn–O bond formation and reduced hydroxyl/carbonyl signals, indicating coordination between Zn^{2+} ions and phytochemical functional groups.

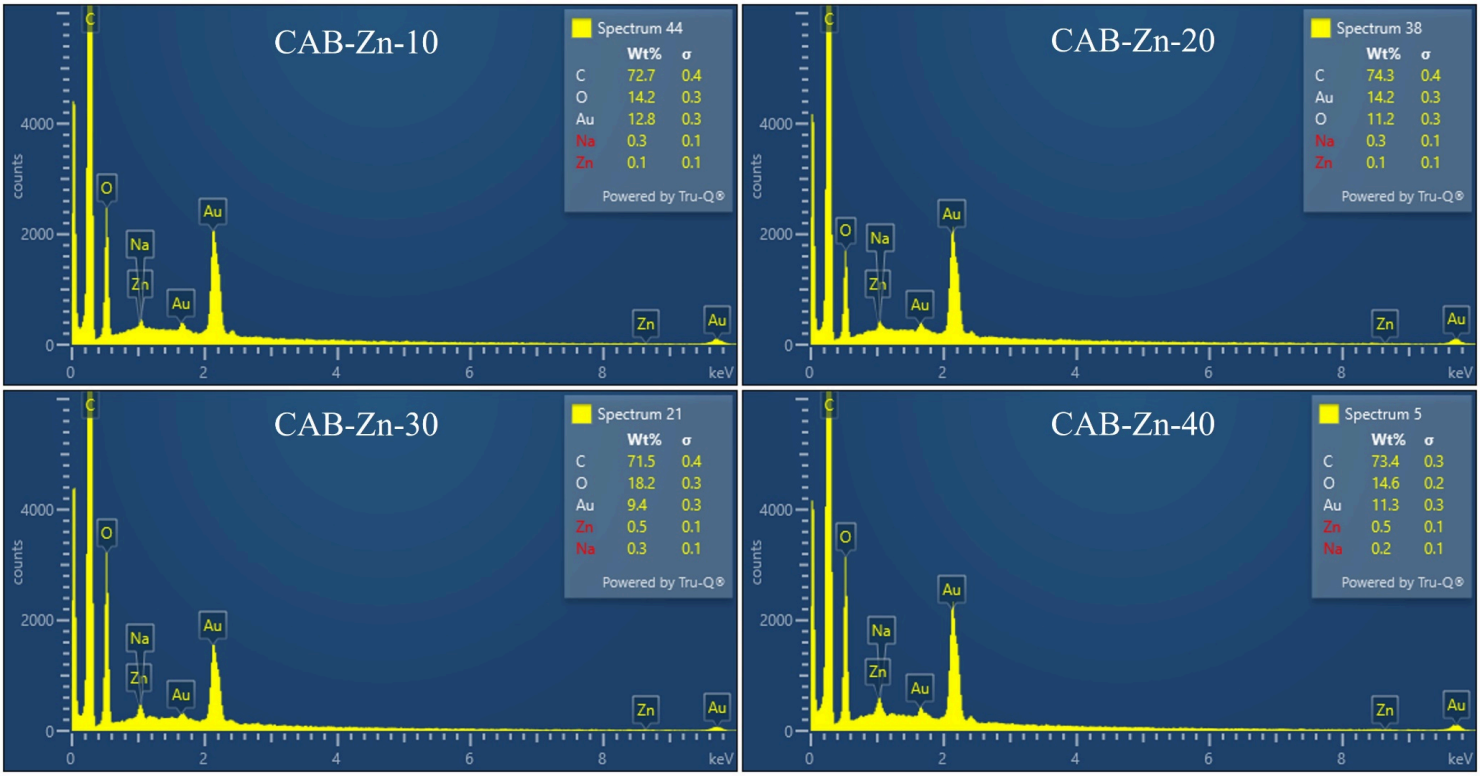

Figure 5

EDS spectra of $Zn(OH)_2$-coated *C. odorata* microcapsules. Detected elements include carbon (C), oxygen (O), and zinc (Zn), with gold (Au) from sputter coating. The increasing Zn signal with higher precursor concentrations confirms controlled and reproducible surface deposition of $Zn(OH)_2$.

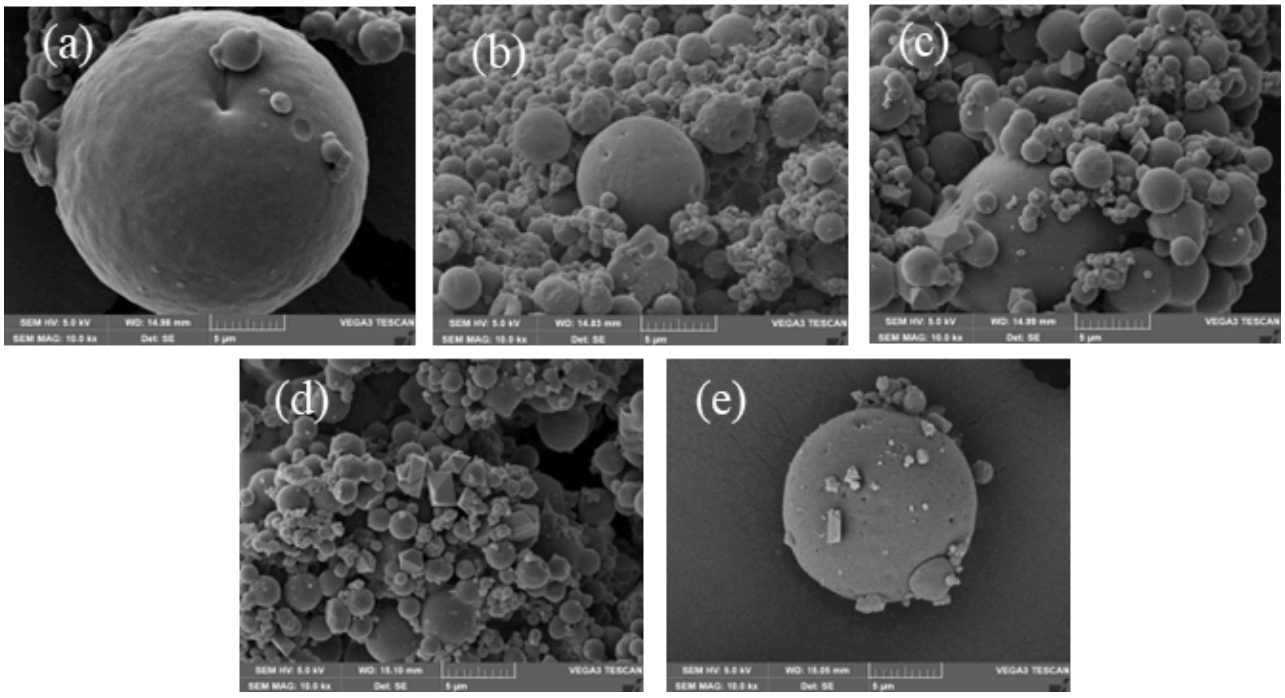

Figure 6

SEM micrographs showing the surface morphology of CAB microcapsules coated with increasing $Zn(OH)_2$ concentrations: (a) CAB-Zn-0 (uncoated), (b) CAB-Zn-10, (c) CAB-Zn-20, (d) CAB-Zn-30, and (e) CAB-Zn-40. Increasing surface roughness and nanoparticle coverage with higher $Zn(OH)_2$ precursor concentrations indicate successful layer formation and suggest improved antimicrobial surface functionality.

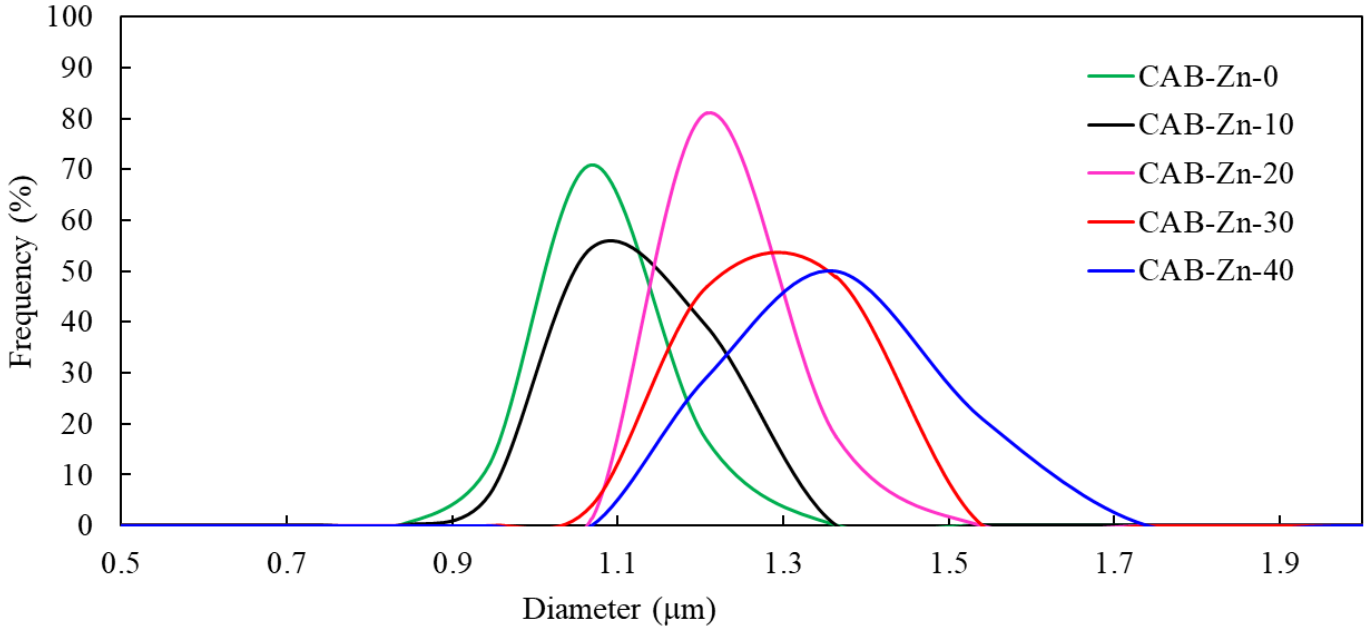

Figure 7

Particle size distribution profiles of CAB microcapsules coated with increasing $Zn(OH)_2$ concentrations. Higher Zn precursor levels result in larger and more uniform microcapsules, supporting enhanced controlled-release behavior.

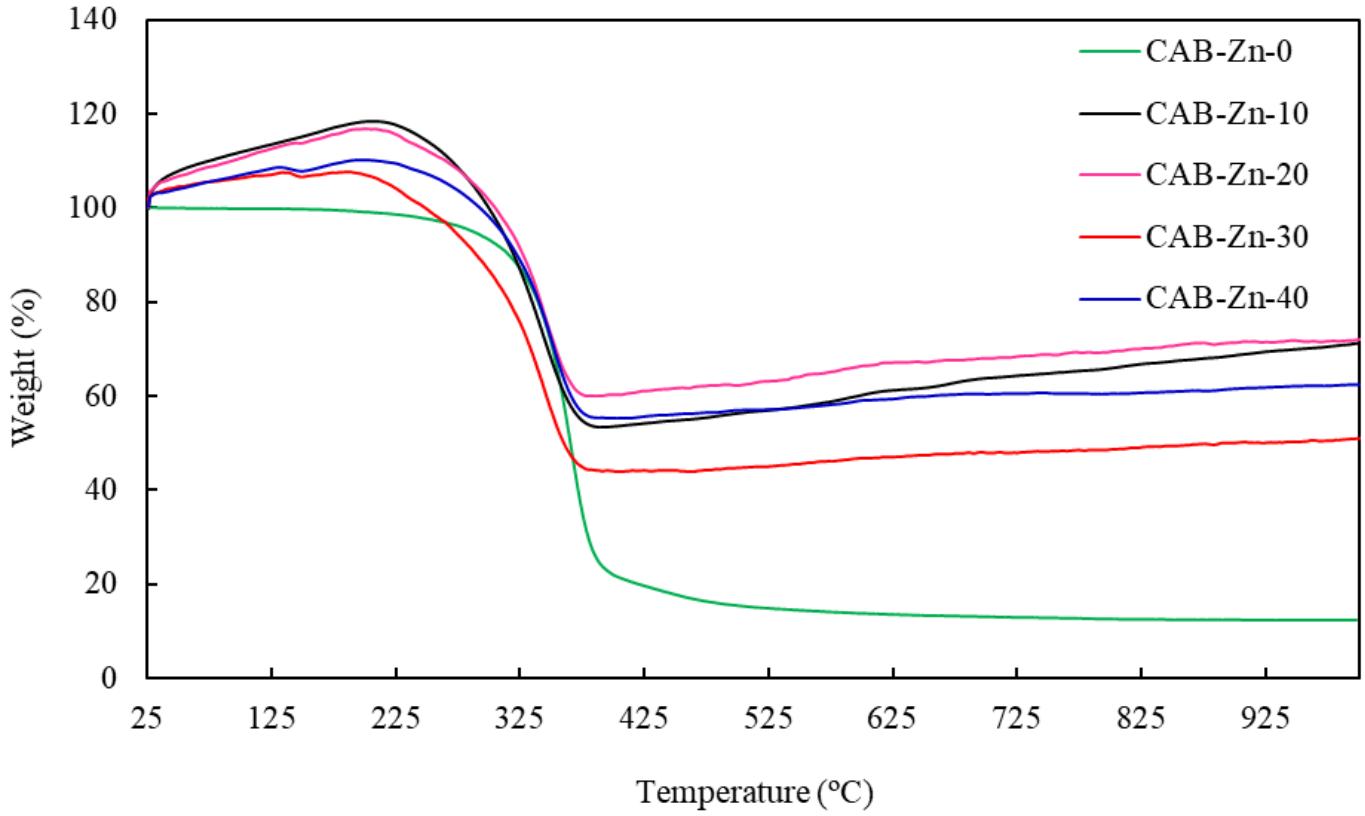

Figure 8

TGA thermograms of CAB microcapsules with and without $Zn(OH)_2$ coatings. Coated formulations demonstrate reduced weight loss and improved thermal stability, confirming the protective role of $Zn(OH)_2$ in preserving structural integrity and phytochemical content during thermal stress.

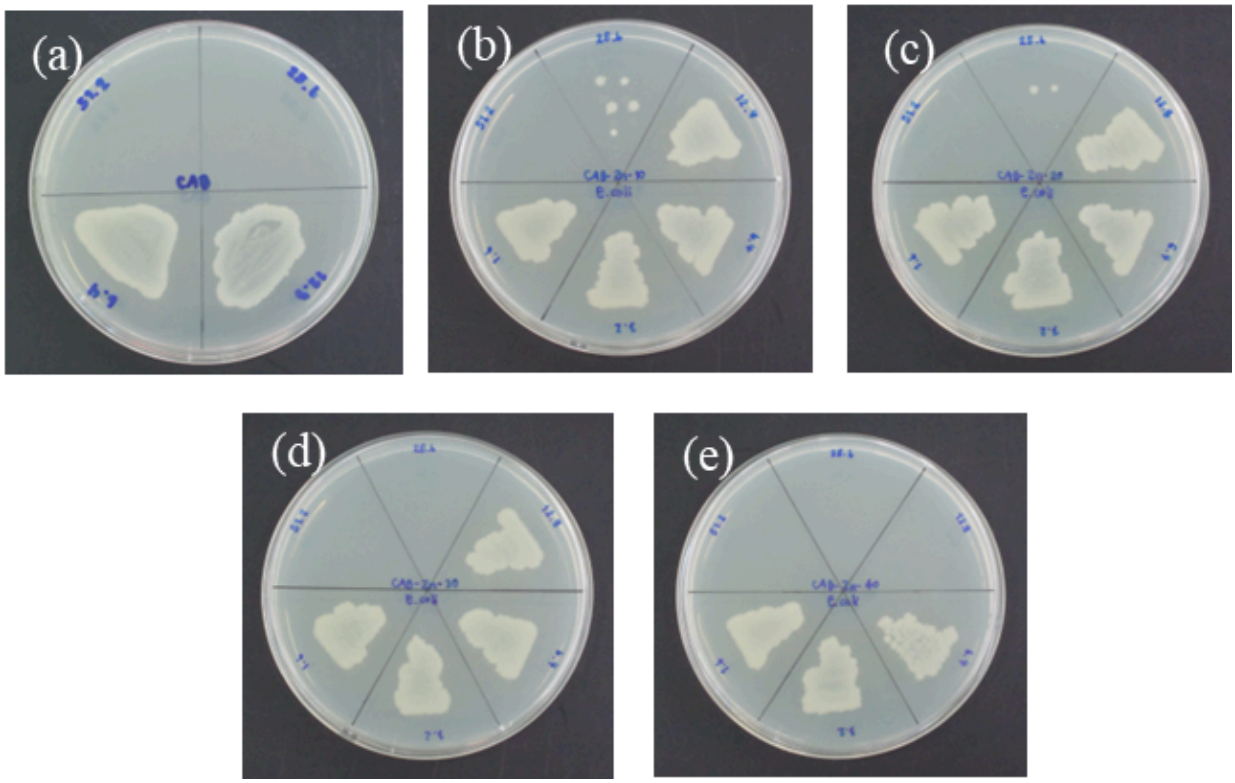

Figure 9

Minimum inhibitory concentration (MIC) values for CAB microcapsules with varying $Zn(OH)_2$ concentrations against *E. coli* and *S. aureus*. Enhanced antibacterial activity is observed with increasing $Zn(OH)_2$ loading, with CAB-Zn-40 exhibiting the lowest MICs.

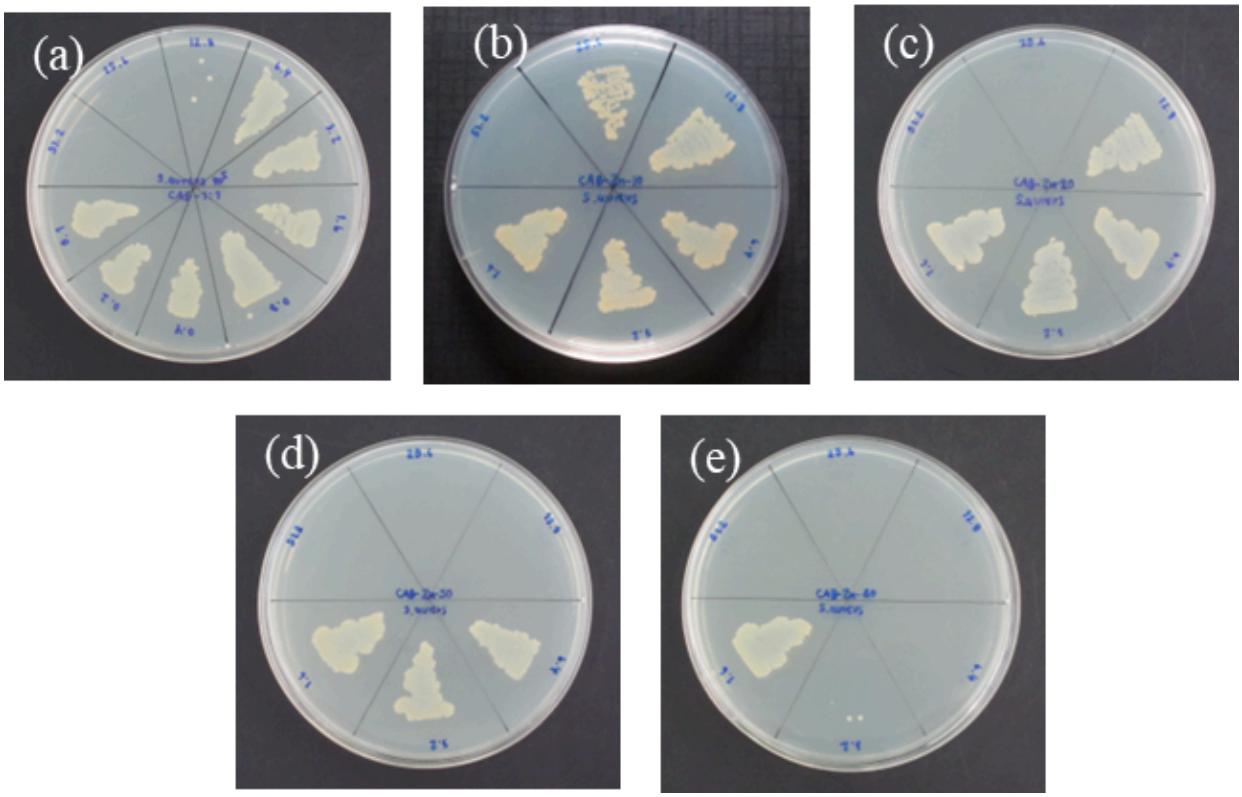

Figure 10

Representative spread plate images illustrating the bactericidal activity of $Zn(OH)_2$-coated microcapsules against *S. aureus*. CAB-Zn-40 achieves complete colony inhibition at low concentrations, confirming potent antimicrobial action.

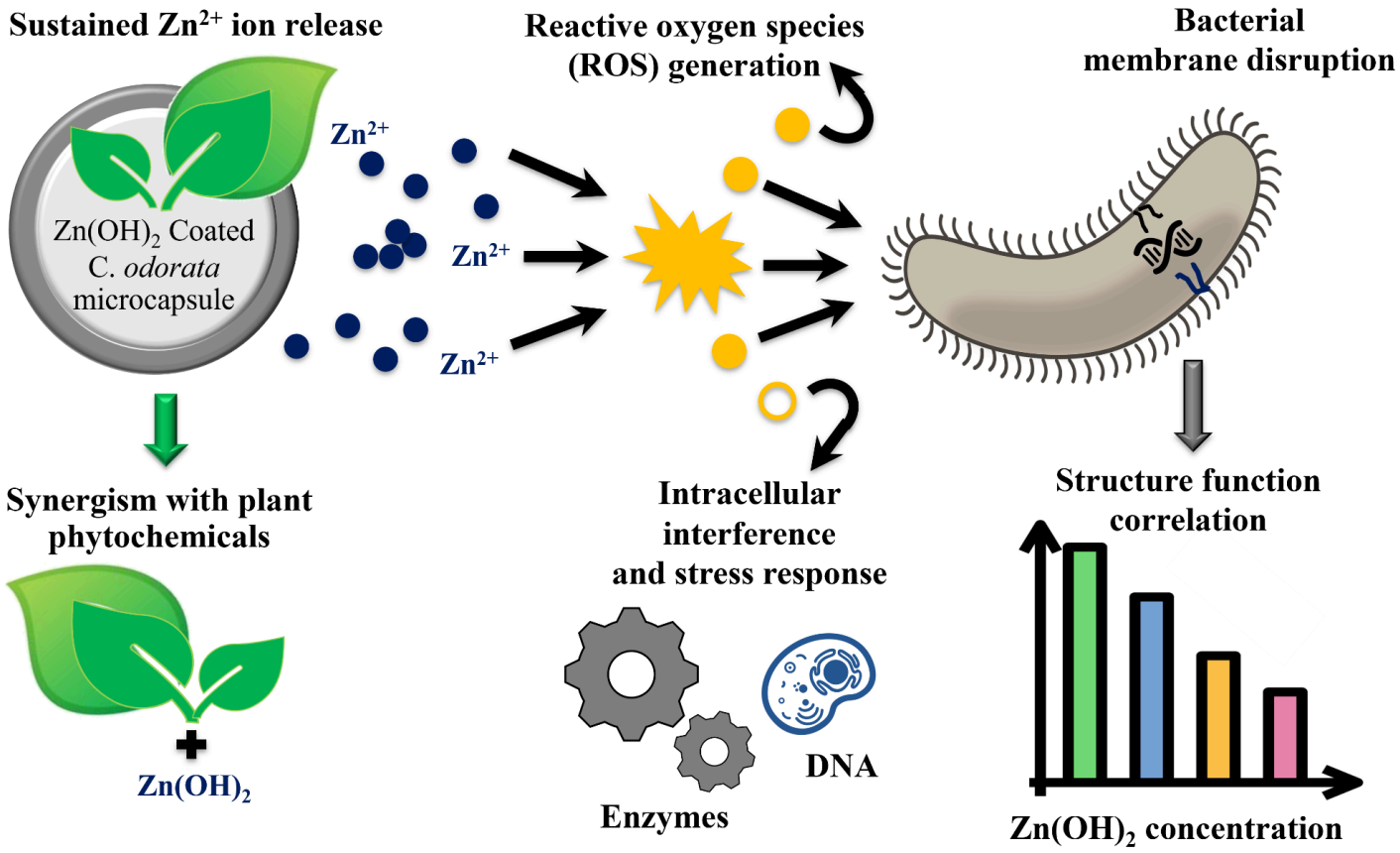

Figure 11

Proposed antibacterial mechanism of $Zn(OH)_2$-coated CAB microcapsules. Sustained Zn^{2+} ion release and ROS generation disrupt bacterial membranes, induce oxidative stress, and interfere with intracellular processes. Phytochemicals from *C. odorata* act synergistically, enhancing antimicrobial efficacy.